YUGATO

ISSN: 0387-5695, eISSN: 0387-5695
Vol. 75 No. 2 (2023)

Received: October 16, 2023 / Revised: November 11, 2023 / Accepted: November 29, 2023 / Published: December 16, 2023

EXPLORING THE MOLECULAR INTERACTION OF BETA-LACTOGLOBULIN WITH TARTRAZINE: A DETAILED SPECTROSCOPIC AND MOLECULAR DOCKING STUDY

S. Gayathri[1] and S. Bakkialakshmi[1*],

[1]Department of Physics, Annamalai University, Annamalai Nagar,
Tamil Nadu, India.

*Corresponding author E-mail: bakkialakshmis@rocketmail.com

ABSTRACT

This study investigated the interaction between the whey protein Beta-lactoglobulin (BLG) and the food colorant tartrazine (TART). This study used techniques such as UV-vis absorption spectroscopy, fluorescence spectroscopy, Fourier transform infrared (FT-IR) spectroscopy, and molecular docking to investigate these interactions. The results showed that the quenching of BLG emission by TART was due to the formation of a ground-state complex (BLG-TART) with substantial binding affinity. Steady-state emission and time-resolved fluorescence studies provided insights into this binding process. According to Förster's theory of non-radiative energy transfer, the average distance at which binding occurs (r) between beta-lactoglobulin (BLG) and tartrazine (TART) was evaluated and analyzed to interpret changes in the secondary structure of BLG using Fourier transform infrared spectroscopy (FTIR). Furthermore, molecular docking studies revealed that hydrogen bonds and hydrophobic forces played a significant role in stabilizing the BLG-TART complex. These results may be beneficial for developing a better understanding of the interactions between food additives and proteins, which could have implications for the food industry and related fields.

Keywords: Tartrazine, Food dye, Beta-lactoglobulin, Binding mechanism, Molecular docking

INTRODUCTION

Beta-lactoglobulin (BLG) is a globular protein present in cow's milk and other animals such as sheep, horses, and pigs. BLG constitutes approximately 10–15% of the total milk proteins. It is a high-quality whey protein isolate with excellent nutritional value[1]. The molecular weight of BLG is 18.4 kDa, and it contains 162 amino acids[2]. BLG has numerous applications in the food and pharmaceutical industries, such as in baked goods, sports nutrition, salad dressings, emulsifiers, medical nutritional formulas, and infant formulas. Its high biological and nutritional qualities make it a suitable candidate for such applications. Research conducted by Tai et al. revealed that BLG has a significant impact on enhancing immune responses by improving cell proliferation via the Immunoglobulin M (IgM) receptor[3].

Food coloring or color additives are substances that are added to food and beverages to give them a specific color. These additives can include dyes, pigments, or chemicals that enhance the visual appeal of various food products, compensate for natural color variations, and ensure consistent coloring. Sensory quality assessment has long considered food coloring an essential aspect. Owing to changing lifestyles and the rise of urbanization, the demand for ready-to-eat processed foods has increased rapidly. Color additives are crucial for maintaining the visual appeal of these products and preventing color loss during storage[4].Tartrazine, also known as FD&C Yellow No. 5, is an anionic, water-soluble, synthetic monoazo dye. It is commonly used as a certified food colorant and found in a wide range of food and pharmaceutical products. Interestingly, tartrazine retains its color

even under high-temperature and acidic conditions. The Joint FAO/WHO Expert Committee on Food Additives (JECFA) established an acceptable daily intake (ADI) of 0-10 mg/kg body weight per day for tartrazine. While it is primarily used in food products such as ice cream, confectionery, soft drinks, and breakfast cereals, it is also commonly found in pharmaceuticals [5].Tartrazine and its metabolites have been found to induce cytotoxicity and genetic damage in human blood lymphocytes, as reported in literature [6]. Azo dyes, such as ponceau, red 40, sunset yellow, and tartrazine, have been associated with genotoxicity in the mouse bone marrow, as detected by the micronucleus assay [7]. In vitro evaluations revealed significant cytotoxicity in human stomach and rat fibroblast cell lines. Additionally, tartrazine has been found to interact with serum proteins such as human serum albumin (HSA) and bovine serum albumin (BSA), leading to amyloid fibril formation. This is of particular concern because amyloid fibrils play a role in the pathogenesis of various neurodegenerative diseases. Tartrazine and its metabolites can enter the bloodstream and bind carrier proteins [8].The nutritional and functional value of BLG is now generally acknowledged and it is commonly utilized as a premium ingredient in contemporary beverages and foods [9]. However, as a food additive, BLG may interact with other food colors and affect their performance.

This study investigated the interaction between the TART dye and whey protein (BLG). Both these components are present in food chain systems. Steady-state fluorescence quenching was used to analyze the in vitro interactions between the TART dye and BLG. Binding constants were calculated in a phosphate buffer (pH 7.4) solution. Conformational changes in BLG were studied using synchronous fluorescence spectra (SFS), and Förster's energy transfer theory was used to determine the distances between BLG as the donor and TART as acceptors. Time-resolved studies were conducted to explore the mechanism of interaction between the dye and whey protein. Molecular docking studies with BLG were performed to confirm the findings of in vitro studies. The presence of tartrazine was detected by FTIR as a conformational change in the secondary structure of BLG. This study offers comprehensive information on the structural changes that occur in dairy proteins owing to their interactions with food additive dyes.

2.MATERIALS AND METHODS:

2.1 Reagents and chemicals

Beta-lactoglobulin (purity ≥ 90%), tartrazine (dye content, 85-95, & phosphate buffer (pH 7·4) were procured from Sigma Aldrich Company, Bangalore. All the reagents used in this study were of analytical grade. Phosphate buffer and distilled water were used as solvents throughout the study.

2.2 Stock solution preparation

BLG stock solution (1×10^{-5} M) was prepared in 1 M phosphate buffer (i.e., physiologic pH 7.4
7.4). The TART dye (1×10^{-5} M) was dissolved in distilled water. All stock solutions were freshly prepared**.**

2.3 UV-Visible spectroscopic analysis

Absorption measurements were carried out using UV-visible spectrophotometer Shimadzu –
UV 1800. The spectra of the prepared solutions were recorded over the wavelength range of 200–800 nm using a quartz cell with an optical path length of 1 cm.

2.4 Steady-state fluorescence spectroscopy

A Shimadzu (Shimadzu Corporation, model RF-5301PC) spectrofluorometer was used to obtain the steady-state fluorescence spectra. Intrinsic fluorescence spectroscopy of BLG with different concentrations of TART was

performed by scanning emission wavelengths in the range of 250–500 nm with an excitation wavelength of 282 nm. The excitation and emission slit widths were kept at 5.0 nm.

2.5 Time-resolved fluorescence measurements

Fluorescence lifetime intensity decay measurements were carried out using a Fluorolog- FL3-11 spectrofluorometer equipped with a time-correlated single-photon counting method with a nano-LED source (Jobin Yvon) used as the excitation source. The fitting of the decays was based on the residual function and the χ^2 value.

2.6 Synchronous fluorescence spectroscopy

Synchronous fluorescence spectra of BLG in the presence of increasing TART concentrations were recorded using an RF-5301PC spectrofluorometer. The concentration was the same as that used for the fluorescence measurements. To assess changes in the microenvironment of tyrosine and tryptophan residues in biomolecules. The $\Delta\lambda$ values were fixed at 15 nm and 60 nm.

2.7 FTIR measurements

FTIR spectra of BLG and BLG-TART samples in the range from 4000 to 400 cm^{-1} with a resolution of 4.0 cm^{-1} were recorded using a Perklin Elmer spectrometer. The FTIR acquisition used ethanol instead of H_2O as the solvent to prepare the sample to reduce the interference of the solvent with the measurement results.

2.8 Molecular docking

The molecular docking of TART binding to BLG was performed using AutoDock 1.5.6 software, which was downloaded from the SWISS-MODEL Repository (http://autodock.scripps.edu/).

2.8.1 Protein structural preparation

For docking simulations, the three-dimensional coordinates of BLG were extracted from its X-ray crystal structure (PDB ID: 3NPO resolved at 2.20 Å) available in the RCSB database. The protein X-ray crystal structure refinement process was prepared by removing nonessential water molecules and optimizing polar hydrogen atoms, and the Kollman charges were assigned using Auto dock. A grid box with dimensions of 40 × 40× 40 Å was generated, as the whole active site cavity of BLG was embedded in it, with a default grid spacing of 0.375.

2.8.2 Ligand structural preparation

A two-dimensional crystal structure of TART (CID: 164825) was downloaded from the National Centre of Biological Information (PubChem database). Tartrazine was considered flexible for docking. Nonpolar hydrogens were merged, Gasteiger charges were imposed, aromatic carbons and rotatable bonds were counted, and TORSDOF was determined and converted to PDBQT (Protein Data Bank, Partial Charge (Q), and Atom Type (T)) file format using Auto Dock Tools version 1.5.6.

2.8.3 Docking protocol

The Lamarckian Genetic Algorithm (LGA) was executed for flexible ligand-protein docking. BLG was considered rigid, and the input torsion roots of the flexible TART ligand were set. Parameters such as the maximum number of 2.5×10^6 energy evaluations, population size of 150, and maximum number of 27,000 generations were performed with 10 genetic algorithm (GA) runs, and other parameters were set as default. The stable conformation of the docked complexes with the lowest binding energy was visualized using PYMOL and BIOVIA Discovery Studio.

3. RESULTS AND DISCUSSION

3.1 UV-Vis absorption spectral studies

UV-visible absorption spectroscopy is a widely used technique for investigating structural changes in proteins and their interactions with ligands. This method is simple yet fundamental, providing valuable insights into complex formation between biomolecules [10]. Fig. 1(a) shows UV–Vis absorption spectra of the BLG-TART complex. A fixed concentration of BLG (0.2X 10^{-5} ml) was titrated without and with an increasing concentration of TART.

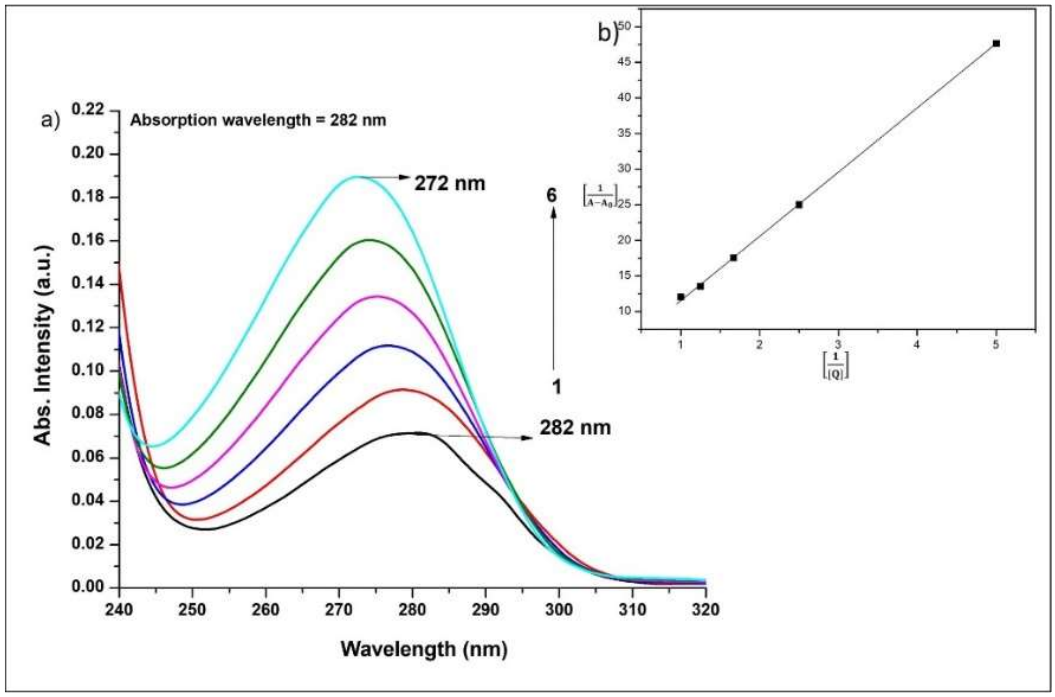

Fig.1. (a) UV-Vis absorption spectra of beta lactoglobulin with different concentrations of tartrazine (mol L^{-1}) (1) 0.0, (2) 0.2, (3) 0.4, (4) 0.6, (5) 0.8 & (6) 1.0. **(b).** The inset panel presents the plot of $\frac{1}{A-A_0}$ versus $\frac{1}{[Q]}$ for BLG with TART.

Fig. 1(a). depicts the absorbance maxima of BLG at 282 nm owing to the presence of aromatic amino acid (tryptophan and tyrosine) residues [11]. Upon increasing the concentration of tartrazine in the solution, a notable increase in the absorption intensity of the peak at 282 nm was observed. This increase led to a significant blue shift in the excitation maxima from 282 to 272 nm, indicative of the formation of a new BLG-TART complex. The change in λ_{max} indicates a shift in polarity around the tryptophan residue, causing a change in the peptide strand of beta-lactoglobulin molecules, resulting in a change in hydrophobicity. Thus, it can be concluded that the binding mechanism between tartrazine and proteins involves intricate structural changes in the protein and its surrounding environment.This result suggested that the interaction between TART and BLG altered the microenvironment of amino acid residues in BLG These findings align with previous studies conducted on the binding between tartrazine and bovine serum albumin, which reported similar outcomes [12] .BLG-TART complex formation can be determined from the following equations:

BLG + TART ⇌ BLG: TART (1)

$$K = \frac{[\text{BLG: Tartrazine}]}{[\text{BLG}]\,[\text{Tartrazine}]} \quad (2)$$

Where K is the binding constant

Assuming, [BLG: TART] = C_B

$$K=\frac{C_B}{[C_{BLG}-C_B]\,[C_{TART}-C_B]} \quad (3)$$

Where C_{BLG} and C_{TART} are the analytical concentrations of BLG and TART in the solution, respectively. According to Beer-Lambert's law

$$C_{BLG}=\frac{A_0}{\varepsilon_{BLG}.1} \quad \text{and} \quad C_{BLG}=\frac{A-A_0}{\varepsilon_B.1} \quad (4)$$

Where A_0 and A absorbance of BLG in the absence and presence of TART, respectively. ε_{BLG} and ε_B are the molar extinction coefficients of BLG and TART, respectively. One shows the light path of the cuvette (1 cm). By displacing equation (3) by equation (4), equation (5) can be deduced:

$$\left(\frac{A}{A-A_0}\right)=\left(\frac{\varepsilon_{BLG}}{\varepsilon_B}\right)+\left(\frac{\varepsilon_{BLG}}{\varepsilon_B}\right).K\frac{1}{C_{TART}} \quad (5)$$

As a result, the graph of $1/(A-A_o)$ versus 1/ [tartrazine] yields a linear delineation in Fig.1(b). Thus K=3.65 x 10^4 (L mol^{-1}) can be calculated by dividing the intercept by the slope with a linear regression coefficient R^2=0.99.

3.2 Fluorescence quenching study of BLG by tartrazine

Tryptophan, tyrosine, and phenylalanine are among the amino acid residues in proteins that can produce protein-intrinsic fluorophores that produce intrinsic fluorescence at a specific excitation wavelength [13]. They have been widely explored for tracking changes in protein structure because they are extremely sensitive to the polarity of the microenvironment. The binding mechanisms, binding constants, and binding sites between BLG and TART were determined by fluorescence spectroscopy. The fluorescence emission spectra of BLG with various TART concentrations at 298 K are shown in Fig.2(a). They have been widely explored for tracking changes in protein structure because they are extremely sensitive to the polarity of the microenvironment. The binding mechanisms,

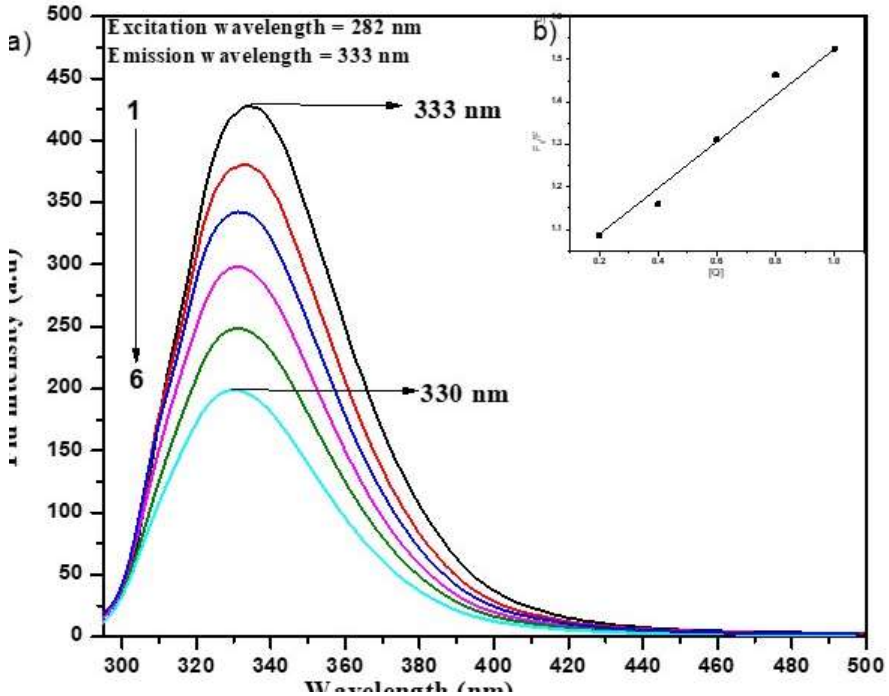

binding constants,and binding sites between BLG and TARTwere determinedd by fluorescence spectroscope. The fluorescence emission spectra of BLG with various TART concentrations at 298 K are shown in Fig.2(a). Under physiological conditions, Beta-lactoglobulin (BLG) emits strong fluorescence at 333 nm when excited at 282 nm, which is consistent with previous reports works in the literature [14]. This intrinsic fluorescence was

due to the presence of Trp residues. The addition of TART to a fixed concentration of BLG decreased the BLG fluorescence intensity.

Fig.2. (a) Steady-state fluorescence spectra of beta lactoglobulin with different concentrations of tartrazine (mol L^{-1}) (1) 0.0, (2) 0.2, (3) 0.4, (4) 0.6, (5) 0.8, and (6) 1.0. **(b)** The inset panel shows the Stern-Volmer plot for BLG with TART.

The peak maximum of the BLG fluorescence shifted from 333 nm to 330 nm as the concentration of TART increased from 0 to 1.0 M. This shift was accompanied by a 3 nm blue shift in the emission wavelength, which was attributed to changes in the hydrophobic cavity of tryptophan upon binding to TART. These changes resulted in decreased hydrophobicity and microenvironmental changes around the tryptophan residues. These findings suggested that TART interacts with BLG and reduces its inherent fluorescence. A similar observation was made regarding the binding interaction of tartrazine with serum albumin [8].

For a quantitative analysis of the quenching mechanism of TART with BLG, the fluorescence quenching process was studied using the Stern–Volmer equation.

$$\frac{F_0}{F} = 1 + k_q\tau_0[Q] = 1+K_{sv}[Q] \quad (6)$$

Where F_0 and F represent the fluorescence emission intensities in the absence and presence of tartrazine (quencher), respectively. K_q is the quenching constant for steady-state fluorescent biomolecules, which was calculated using the following (Eqn.6).

$$k_q = \frac{K_{sv}}{\tau_0} \quad (7)$$

where τ_0 is the average lifetime of BLG (τ) obtained from a time-resolved fluorescence study, K_{sv} is the Stern–Volmer (SV) quenching constant, and [Q] is the concentration of tartrazine. The Stern–Volmer plot was linear (Fig. 2b), with K_{sv}= 1.092 × 10^5 (L mol^1). This indicates that the azo dye tartrazine has strong quenching ability. The value of K_q was found to be 2.83 x 10^{13} (L mol^1S^{-1}). According to Lakowicz, the dynamic fluorescence quenching mechanism occurs when the maximum quenching constant K_q in an aqueous solution is 1 × 10^{10} [M^{-1} s^{-1}] [15]. The obtained K_q value is greater than the maximum value possible for a dynamic process, revealing that the quenching mechanism is static in nature and forms a ground state complex between BLG-tartrazine. The creation of a non-fluorescent fluorophore-quenching combination is referred to as static quenching. The calculated correlation coefficient of the SV plot is R^2=0.99. This further supports the dominance of a static quenching mechanism in fluorophore-quencher systems [16].

where τ_0 is the average lifetime of BLG (τ) obtained from the time-resolved fluorescence study, K_{sv} is the Stern–Volmer quenching constant, and [Q] denotes the concentration of tartrazine. The Stern–Volmer equation plot of BLG fluorescence quenched by varying concentrations of TART is shown in Fig.2(b). Thus, the Stern–Volmer quenching constant K_{SV} was obtained from the slope of F_0/F against [Q] in the linear range, and K_q was also calculated, reflecting the binding affinity between the protein (BLG) and the quencher (TART), with higher values representing a stronger binding affinity, effectiveness of quenching, or the accessibility of the fluorophore to the quencher. According to the Stern-Volmer plot, a single quenching mechanism, either static or dynamic, is represented by a linear plot. By analyzing the slope of the linear function of F_0/F versus the quencher concentration [Q], one can determine the necessary values for K_{sv}, which is equal to 5.01 x 10^4 L mol^{-1}.K_q is as high as 2.83 x 10^{12} $M^{-1}s^{-}1$. The calculated Kq from the Stern-Volmer curve equation was three orders higher than the limiting

diffusion rate constant of the biomolecules (2×10^{10} $[M^{-1} s^{-1}]$)[17], indicating that static quenching was the main quenching mechanism between BLG and TART and was not dynamic.

3.3. Binding Constant and Binding sites

The binding constant and binding sites for the interaction of BLG with tartrazine can be obtained from the double-logarithm equation (8)

$$\log\left[\frac{F_0-F}{F}\right] = logk_b + nlog[Q] \quad (8)$$

$\log\left[\frac{F_0-F}{F}\right]$ is plotted against $\log[Q]$ (Fig.3.) and the slope obtained from the plot gives the number of binding sites (n) and intercept yields the value of binding constant K_a

The binding free energy can be calculated using Eqn.9.

$$\Delta G = -2.303RTl_nK_a \quad (9)$$

Where R is the gas constant and T is the temperature(298 K).

The values of K_a (binding constant) and n (number of binding sites) were determined to be 5.7×10^5 L mol-1 and 1.4, respectively, with a high degree of correlation ($R^2 = 0.99$). The study of the BLG-TART complex indicated that the binding of TART to BLG is a spontaneous process, as the complex exhibits a negative free energy (ΔG) value of -74.95 KJ mol-1. The K_a value, which measures the efficiency of protein interactions, ranges from to 10^3-10^6 M-1, suggesting that the BLG-TART complex has a highly efficient interaction with the protein [18].

These findings are supported by negative ΔG values, which indicate that the binding of TART to BLG is energetically favorable.

Fig.3. Double log plot of beta lactoglobulin with tartrazine

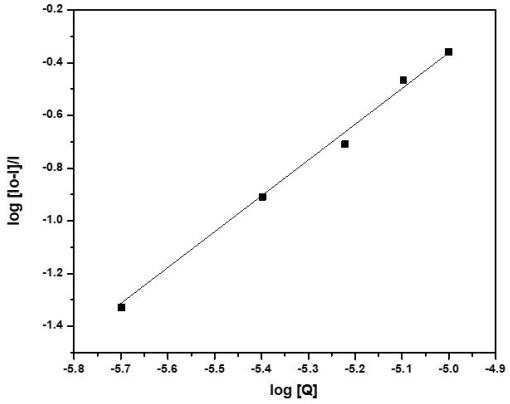

3.4. Synchronous fluorescence spectroscopy

To provide information on polarity changes in the chromophore's surroundings, synchronized fluorescence spectroscopy is frequently employed to analyze conformational changes in protein structure. Tryptophan residues of BLG, can be seen in the synchronous fluorescence spectrum when Δλ is set to 60 nm. When the wavelength is tuned to Δλ =15 nm, one may a unique peak of tyrosine residues in the proteins may be observed. The change in polarity of the local environment is determined by the change in the maximum emission [31]. The synchronous fluorescence spectra of BLG and the complex upon addition of TART are displayed in Fig. 4(a) and 4(b).

Fig. 4. Synchronous fluorescence spectra of beta-lactoglobulin with tartrazine at **(a)** Δλ=15 nm and **(b)** Δλ=60 nm.

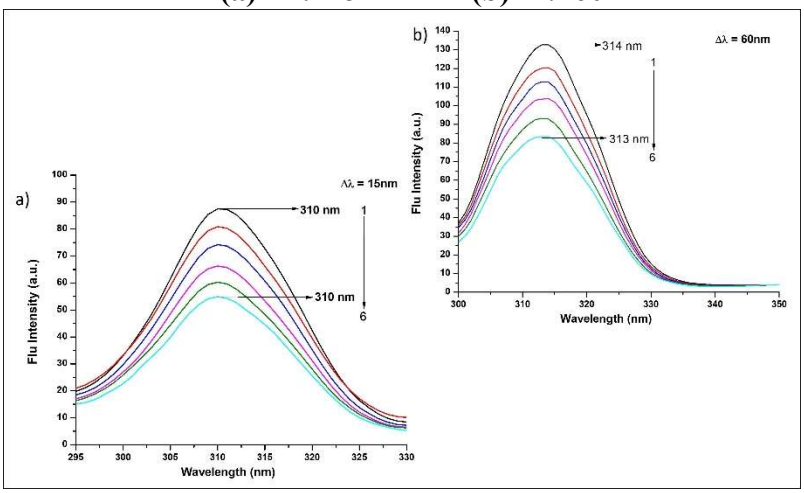

As illustrated in Fig.4, the addition of TART to BLG resulted in a significant reduction in the fluorescence intensity of amino acids Tyr and Trp. Interestingly, Trp was more susceptible to the quenching effect of TART than Tyr. These findings suggest that TART causes a transformation in the conformational structure of BLG, leading to the exposure of Trp residues. This exposure of Trp residues was the main cause of quenched intrinsic fluorescence, as Trp is exceptionally sensitive to changes in the polarity of its surrounding environment [19].The Fig .4(b) indicates that the presence of TART caused a blue shift of 1 nm in the maximum emission peak of Trp residues, indicating an increase in hydrophobicity and a decrease in polarity of the microenvironment of Trp due to the BLG-TART interaction. These findings were in agreement with the results of the fluorescence experiments. During the interaction of TART with BLG, a regular decrease in tyrosine fluorescence emission was observed. However, there was no notable change in the wavelength. This indicates that the conformation of the tyrosine microregion remains unaffected by the interaction between TART and BLG. Synchronous fluorescence spectroscopy results indicated that the BLG-TART complex involves a hydrophobic interaction between tartrazine and BLG, and the amino acid residues on BLG form stable complexes with the aromatic groups of the azo dye. These findings indicate that tartrazine has an impact on the microenvironment around tryptophan residues that surround BLG. This interaction modifies the conformation of BLG. However, the binding of TART to BLG did not affect the conformation of the tyrosine microregion. Similar findings were reported for the interaction of Sudan III with bovine serum albumin [20].

3.5. Time resolved fluorescence studies

3.5. Time resolved fluorescence studies

According to Lakowicz's theory, static and dynamic processes can be easily distinguished by fluorescence quenching obtained from time-resolved fluorescence measurements [29]. While dynamic quenching causes significant changes in the fluorescence lifetime, static quenching is characterized by stable fluorescence lifetime values. The fluorescence decay of free BLG and the protein with ligand (BLG + TART) addition is illustrated in Fig. 5. The fitted results are presented in Table 1.

Fig.5. Time-resolved fluorescence decays of beta lactoglobulin in phosphate buffer (pH=7.4)with different concentrations of tartrazine (1) 0.0, (2) 0.4, and (3) 0.8 (mol l^{-1}).

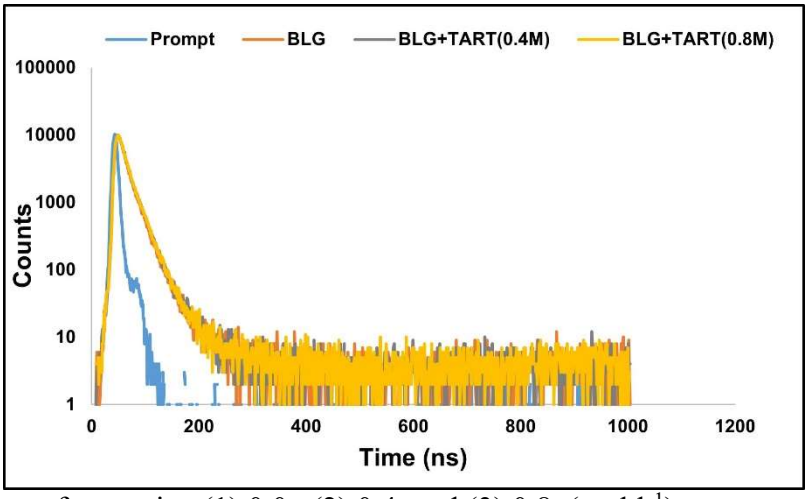

Fig.5 displays representative fluorescence decay images of beta-lactoglobulin at different molar ratios of tartrazine in phosphate buffer with a pH value of 7.4. Table 1 shows the fluorescence lifetime and amplitude measurements for the same samples. The value of $\chi 2$ is the Durbin−Watson parameter (greater than 1.7), indicating goodness of fit [21,22]. The decay curves were accurately fit to a tri-exponential function, revealing an emerging relative fluorescence lifetime of $\tau_1 = 0.93$ ns, $\tau_2 = 3.15$ ns and $\tau_3 = 6.15$ ns of BLG while in the maximum concentration of TART, the lifetime is $\tau_1 = 0.74$ ns, $\tau_2 = 1.83$ ns and $\tau_3 = 4.90$ ns. The independent components were not included. Instead, qualitative analysis was performed using the average fluorescence lifetime. The average lifetime was calculated using Eq. (5).

$$<\tau> = \frac{\alpha_1\tau_1^2 + \alpha_2\tau_2^2 + \alpha_3\tau_3^2}{\alpha_1\tau_1 + \alpha_2\tau_2 + \alpha_3\tau_3} \quad (5)$$

Table1.Fluorescence lifetime and relative amplitudes of beta lactoglobulin with different concentrations of tartrazine

Concentration (M)	Lifetime (ns)			Average life time x 10^{-9} sec	Relative amplitude			χ^2	S.D 10^{-11} sec		
	τ_1	τ_2	τ_3		α_1	α_2	α_3		τ_1	τ_2	τ_3
BLG	0.93	2.11	6.15	1.77	37.64	59.74	2.62	1.20	6.49	3.71	18.34
BLG + TART (0.4M)	0.87	2.01	5.20	1.76	33.68	61.79	4.53	1.17	6.55	4.46	23.25

BLG + TART (0.8M)	0.74	1.83	4.90	1.68	29.21	65.27	5.52	1.22	6.49	3.71	18.34

The average lifetime of beta-lactoglobulin did not change significantly, only from 1.77 to 1.76 ns and 1.68 ns, at different tartrazine concentrations, indicating that fluorescence quenching is essentially a static mechanism. This study indicates that the BLG-TART complex exhibits a static quenching mechanism, which is in line with the outcomes acquired from the SV plot. Furthermore, the fluorescence lifetime of one constituent (τ_1) remained unchanged in all three systems, but the fluorescence lifetime of another component (τ_3) increased when tartrazine was bound to beta-lactoglobulin. This suggests that complex formation between the fluorophore and tartrazine generates a non-fluorescent beta-lactoglobulin-azo dye complex [23].

3.6. Fluorescence resonance energy transfer (FRET) between TART and BLG

FRET is a non-destructive spectroscopic approach used to gauge the proximal distance and relative angular orientation between donor and acceptor molecules [24]. The overlapping fluorescence spectra of BLG (donor) and the UV–Vis absorption spectra of TART(acceptor) are shown in Fig.6. In this instance, TART acts as the acceptor, the tryptophan residue of the BLG protein serves as the donor, and the shaded area delineates the sufficient spectral overlap between the donor and acceptor (Fig.6). .

The following equations determine the energy transfer efficiency (E) in accordance with Forster's nonradiative energy transfer theory:

$$E= 1-\frac{F}{F_0}=\frac{R_0^6}{R_0^6+r^6} \quad (6)$$

$$R_0^6 = 8.79 \times 10^{-25} \times k^2 n^{-4} \varphi J \quad (7)$$

$$J=\frac{\sum F(\lambda)\varepsilon(\lambda)\lambda^4 \Delta\lambda}{\sum F(\lambda)\Delta\lambda} \quad (8)$$

Förster's hypothesis states that the energy transfer efficiency (E) is related to both the distance (r) between acceptor and donor and R_0 the characteristic distance (or Forster radius) with a 50% transfer efficiency. where F and F_0 are the fluorescence intensities of the donor in the presence and absence of the acceptor, respectively; r represents the acceptor-donor distance, where k^2 =2/3 is the spatial orientation factor of the dipole, which is the average value integrated over all possible angles; N is the refractive index of the medium (1.336); Φ is the fluorescence quantum yield of the donor (0.15); and J is the overlap integral of the emission spectrum of the donor

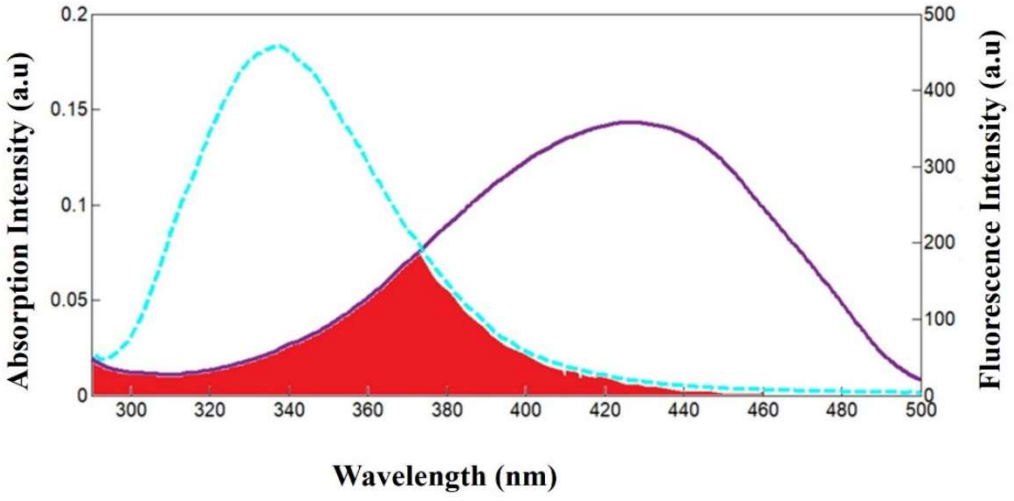

and the absorption spectrum of the acceptor calculated using Eqn.8.F(λ) is the corrected fluorescence intensity of the donor in the wavelength range, from λ to λ + Δλ; ε(λ) is the extinction coefficient of the acceptor at λ. According to Eqn. 6−8. The evaluated parameters are listed in Table 2.

Fig.6. The overlap of UV absorption spectra of tartrazine (solid line) with the fluorescence emission spectra of Beta lactoglobulin (dashed line)

FRET, or Förster resonance energy transfer, plays a crucial role in measuring the distance between molecules. In this context, the overlap region between the donor and acceptor molecules must be less than 8 nm, and typically, r values between 0.5 R_o and 1.5R_o result in a high energy transfer probability. The static quenching observed between BLG and TART suggested the formation of a complex between them. The overlap between the emission spectra of equimolar concentrations of BLG and the absorption spectra of tartrazine indicates good energy transfer efficiency, which was computed within the wavelength range of 300-500 nm. The results of the computation are presented in Table 2, where it is evident that the addition of tartrazine led to a reduction in the fluorescence intensity, which is indicative of Forster energy transfer.

Table 2. Efficiency transfer energy (E) and critical energy transfer distance (Ro) of BLG with TART

Quenchers	Energy(E)	R_o (nm)	J ($cm^{-6}mM^{-1}$) (10^{-15})	r (nm)
Tartrazine	0.30	2.89	7.09	3.31

The interaction between BLG and tartrazine involved a static quenching process that transferred energy without radiation. The distance between the donor and acceptor was measured to be 3.31 nm, which was greater than the maximum critical distance of 2.89 nm. This indicates that the observed quenching process can be attributed to static quenching. The Forster distance (R_o) and donor-acceptor distance (r) obtained from these studies are consistent with previous findings. Efficient energy transfer in beta-lactoglobulin (BLG) depends on the proximity of the donor and acceptor molecules as well as the presence of two tryptophan (Trp) residues. Therefore, both Trp residues must be considered when determining the energy transfer efficiency [25].

3.7.2 Fourier Transform Infrared Spectroscopy

With great sensitivity and specificity, Fourier-transform infrared (FTIR) spectroscopy is a quick and non-destructive technique for identifying alterations in molecular structure. It can be used to distinguish between the different functional groups found in a sample. When FTIR analysis was performed on proteins, nine amide bands, including amide I, II, and III bands, which correlate to various peptide moiety vibration ranges, were found. These bands are particularly helpful for studying protein conformation [26]. FTIR spectroscopy analyzes changes in protein secondary and tertiary structures to identify conformational changes brought about by ligand binding to globular proteins [9]. Using this method, the effect of tartrazine on the secondary structure of BLG protein molecules has been examined; Fig. 7 shows the spectrum region of interest.

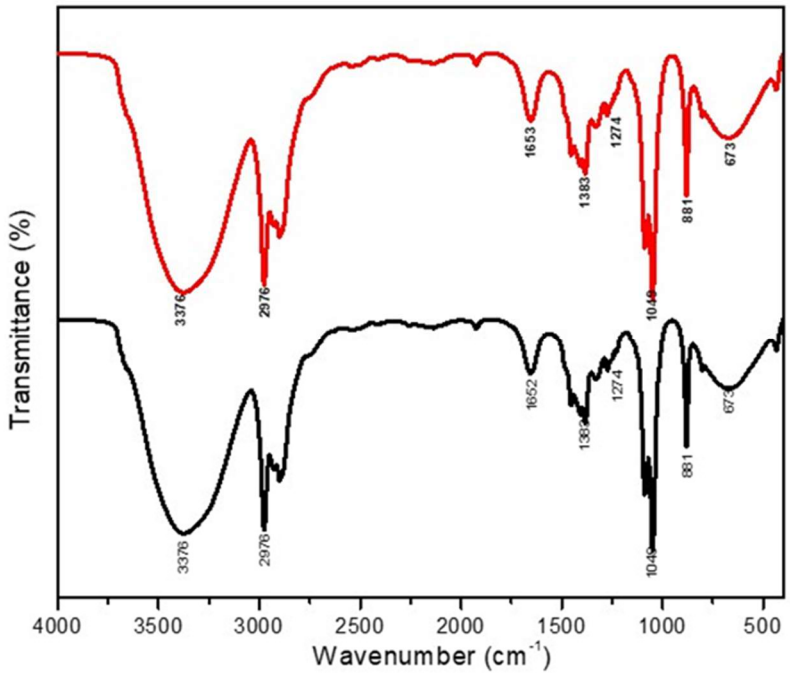

Fig.7.FTIR Spectra of (a) Beta lactoglobulin, (b) Beta lactoglobulin + Tartrazine

The amide band of protein amide I, ranging from to 1700-1600 cm-1, is a result of the degree of hydrogen bonding between the C=O components. The amide I region, which is widely used for protein conformational studies, assigns α-helices between 1649-1658 cm^{-1}, intramolecular β-sheets between 1620-1635 cm^{-1}, and β-turns between 1665-1690 cm^{-1} [27,28].Table 3 shows the FTIR peak assignments of BLG with and without tartrazine. The FTIR spectra of BLG and BLG-Tartrazine complex FTIR tartrazine are shown in Fig. 7. A shift in the amide I band peak location from 1652 cm-1 to 1653 cm-1 is evident. The alterations in these peak positions indicated that the polypeptide carbonyl hydrogen bonding pattern was rearranged as a result of tartrazine interaction with the C =O group in the protein structural subunits [29]. A conformational shift in BLG resulting from the local unraveling of the α-helix into loops is indicated by the slight spectral shift of the amide I band at 1651 cm-1 upon BLG-TART complexation [30]. These results are evident in the changes in the secondary structure of BLG upon binding with tartrazine.

Table.3 FTIR tentative peak assignments of BLG without and with tartrazine

Wavenumber (cm^{-1})		Tentative peak assignments
BLG	BLG+TART	
3376	3376	(N-H Stretching)
2976	2976	CH2 stretching vibrations
1652	1653	(C=O Stretching)
1394	1394	N-H Bending
1331	1331	(C-N stretching)
1274	1274	N-H Bending

1049	1049	C−C and C−OH stretching modes
881	881	C-H Bending vibration
673	673	OCN Bending

3.8. Molecular Docking

In silico docking predicts the optimal orientation of the ligand in the active site of the receptor, and investigates the compatibility between a ligand and a protein target at the molecular level. Beta-lactoglobulin is a single polypeptide chain with 162 amino acid residues. An α-helix and nine anti-parallel β-strands with eight β-sheets were folded into a cone-shaped barrel, forming a hydrophobic pocket constituting the subunit of the core of the BLG structure. The β-strands A–H form a β-barrel, which is the central calyx of the BLG crystal structure; it is the primary binding site of many ligands, especially palmitic acid [31]. The primary binding site was named site 1, located in the internal cavity of the β-barrel, whereas site 2 was identified to be towards the exterior of the β-barrel. These are the two most probable binding sites in BLG [32]. Molecular docking was performed using TART at the primary binding site of BLG, and the results are presented in Fig.8. and Table.4 ,5. It seems that TART fits comfortably in the hydrophobic cavity of the BLG.

The TART-BLG complex could be stabilized by four hydrogen bonds with LYS69(1.77 Å), ASN88 (1.95 Å), ASN90(1.95Å), GLN120(2.80 Å) (Table.4). The BLG-TART complex was further stabilized by four hydrophobic interactions with VAL41(4.67 Å), LEU58 (5.45 Å), ILE7(14.67 Å), ALA86 (5.28 Å).

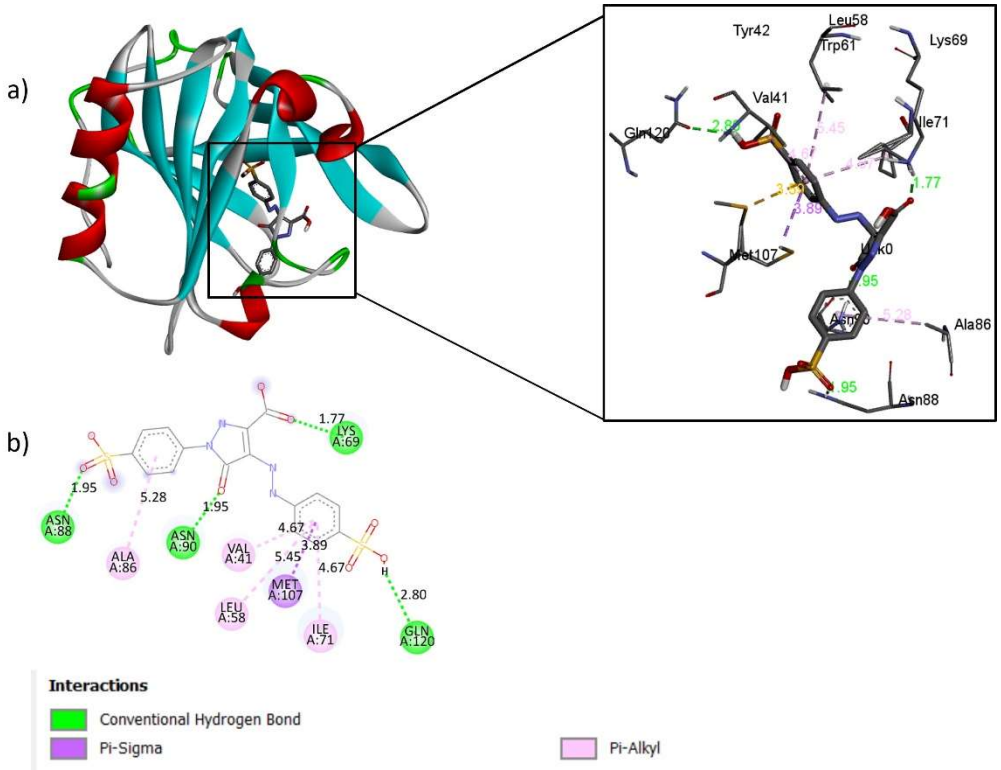

Fig.8. (a)3D molecular docking and **(b)** 3D ligand interaction. **(c)** 2D diagram ligand interaction of beta-lactoglobulin with tartrazine dye.

Table 4. Interacting residues of beta lactoglobulin With tartrazine dye

SI.NO.	Nature of interactions	DISTANCE (Å)	TYPES OF BOND
1.	LYS69	1.77	Hydrogen Bond
2.	ASN88	1.95	Hydrogen bond
3.	ASN90	1.95	Hydrogen bond
4.	GLN120	2.80	Hydrogen bond
5.	MET107	3.89	Hydrophobic(Pi-Sigma)
6.	MET107	3.59	other (Pi-Sulfur)
7.	VAL41	4.67	Hydrophobic (Pi-Alkyl)
8.	LEU58	5.45	Hydrophobic (Pi-Alkyl)
9.	ILE71	4.67	Hydrophobic (Pi-Alkyl)
10.	ALA86	5.28	Hydrophobic (Pi-Alkyl)

The docking results (Table.5) showed that tartrazine had good docking scores with BLG, with a binding energy of -8.22 Kcal/mol. In Fig. 8(b), it can be observed that the ligand is stabilized by four hydrogen bonds involving the D β-strand, F β-strand, Lys69, Asn88, Asn90, and GLN 120 residues. Additionally, π-alkyl interactions between the aromatic ring of tartrazine and Val41, Leu58, and Ala86 residues indicate that the B, C, and E β-strands also contribute to ligand stabilization within the calyx region of β-lactoglobulin [11]. The residue Met107 in the protein points towards the inside and is affected by ligand binding in the central cavity. Additionally, loop EF (residues 85-90) acts as a gate over the central calyx. On one hand, binding within the central cavity was evidenced by the involvement of the calyx entrance with the perturbation of Ly69 and residues around Ile71[33,34].The docking results (Table.5) of hydrophobic interactions and hydrogen bonds have been implicated in the binding of ligands to the hydrophobic cavities of BLG has been reported earlier.

Table.5 Docking results of BLG with tartrazine

DYE	**PROTEIN ID**	**BINDING ENERGY** kcal/mol	**RMSD** A	**INHIBITION CONSTANT** μM	**INTER MOLECULAR ENERGY** kcal/mol	**Vdw+ Hbond+ Desolv Energy** kcal/mol	**ELECTROSTATIC ENERGY** kcal/mol
TART	3NPO	-8.22	5.44	0.94	-10.61	-9.71	-0.89

CONCLUSION

The binding interaction between tartrazine (TART) and beta-lactoglobulin (BLG) has been studied using various experimental techniques. The results showed that TART quenched the fluorescence of BLG via a static quenching mechanism, and the binding process was spontaneous with negative Gibbs free energy. Synchronous fluorescence spectroscopy showed that the polarity around the Tyr and Trp residues of BLG increased upon interaction with TART, indicating a slight change in the conformation of the protein. The distance (r) between nalorphine and the tryptophan residue of BLG was calculated to be 3.31 nm using Förster's theory of non-radiation energy transfer. Changes in the secondary structure of BLG were also observed upon binding to TART, and molecular docking studies confirmed the interaction between the tartrazine molecule and the protein. Understanding the interactions

between food color and proteins is crucial for determining the safety of food dyes. For instance, TART food additives can bind to the BLG protein and induce conformational changes, which have significant implications in food science. These findings highlight the potential toxicity of food dyes and underscore the importance of careful evaluation.

REFERNCES

(1) Guo, M. *Whey Protein Production, Chemistry, Functionality, and Applications*; John Wiley & Sons, 2019.

(2) Al-Shabib, N. A.; Khan, J. M.; Malik, A.; Alsenaidy, M. A.; Rehman, M. T.; AlAjmi, M. F.; Alsenaidy, A. M.; Husain, F. M.; Khan, R. H. Molecular Insight into Binding Behavior of Polyphenol (Rutin) with Beta Lactoglobulin: Spectroscopic, Molecular Docking and MD Simulation Studies. *Journal of Molecular Liquids* **2018**, *269*, 511–520. https://doi.org/10.1016/j.molliq.2018.07.122.

(3) Tai, C. S.; Chen, Y. Y.; Chen, W. L. *β*-Lactoglobulin Influences Human Immunity and Promotes Cell Proliferation. *BioMed Research International* **2016**, *2016*, e7123587. https://doi.org/10.1155/2016/7123587.

(4) Mittal, J. Permissible Synthetic Food Dyes in India. *Reson* **2020**, *25* (4), 567–577. https://doi.org/10.1007/s12045-020-0970-6.

(5) Alsantali, R.; Raja, Q.; Alzahrani, A.; Sadiq, A.; Naeem, N.; Mughal, E.; Al-Rooqi, M.; El Guesmi, N.; Moussa, Z.; Ahmed, S. Miscellaneous Azo Dyes: A Comprehensive Review on Recent Advancements in Biological and Industrial Applications. *Dyes and Pigments* **2021**, *199*, 110050. https://doi.org/10.1016/j.dyepig.2021.110050.

(6) Mpountoukas, P.; Pantazaki, A.; Kostareli, E.; Christodoulou, P.; Kareli, D.; Poliliou, S.; Mourelatos, C.; Lambropoulou, V.; Lialiaris, T. Cytogenetic Evaluation and DNA Interaction Studies of the Food Colorants Amaranth, Erythrosine and Tartrazine. *Food and Chemical Toxicology* **2010**, *48* (10), 2934–2944. https://doi.org/10.1016/j.fct.2010.07.030.

(7) De Souza, C. S. H.; Chapman, J. M.; Da Silva, T. A.; Silva Filho, T. H. N.; Dias, C. T. D. S.; Oliveira, N. D. M. S.; Boriollo, M. F. G. Genotoxic and Cytotoxic Potential of Food Azodyes: Preclinical Safety Assessment Using the in Vivo Micronucleus Assay: Potencial Genotóxico e Citotóxico de Azocorantes Alimentícios: Avaliação de Segurança Pré-Clínica Usando o Ensaio Do Micronúcleo in Vivo. *BJDV* **2022**, 57227–57247. https://doi.org/10.34117/bjdv8n8-158.

(8) Al-Shabib, N. A.; Khan, J. M.; Alsenaidy, M. A.; Alsenaidy, A. M.; Khan, M. S.; Husain, F. M.; Khan, M. R.; Naseem, M.; Sen, P.; Alam, P.; Khan, R. H. Unveiling the Stimulatory Effects of Tartrazine on Human and Bovine Serum Albumin Fibrillogenesis: Spectroscopic and Microscopic Study. *Spectrochimica Acta Part A: Molecular and Biomolecular Spectroscopy* **2018**, *191*, 116–124. https://doi.org/10.1016/j.saa.2017.09.062.

(9) Ramos, Ó. L.; Pereira, R. N. C.; Rodrigues, R. M. M.; Teixeira, J. A.; Vicente, A. A.; Malcata, F. X. *Whey and Whey Powders: Production and Uses*; Elsevier, 2015. https://doi.org/10.1016/B978-0-12-384947-2.00747-9.

(10) Khan, J. M.; Malik, A.; Husain, F. M.; Alkaltham, M. S. Molecular Interaction of Sunset Yellow with Whey Protein: Multi-Spectroscopic Techniques and Computational Study. *Journal of Molecular Liquids* **2022**, *345*, 117838. https://doi.org/10.1016/j.molliq.2021.117838.

(11) Abdollahi, K.; Ince, C.; Condict, L.; Hung, A.; Kasapis, S. Combined Spectroscopic and Molecular Docking Study on the pH Dependence of Molecular Interactions between β-Lactoglobulin and Ferulic Acid. *Food Hydrocolloids* **2020**, *101*, 105461. https://doi.org/10.1016/j.foodhyd.2019.105461.
(12) Leulescu, M.; Rotaru, A.; Pălărie, I.; Moanţă, A.; Cioateră, N.; Popescu, M.; Morîntale, E.; Bubulică, M. V.; Florian, G.; Hărăbor, A.; Rotaru, P. Tartrazine: Physical, Thermal and Biophysical Properties of the Most Widely Employed Synthetic Yellow Food-Colouring Azo Dye. *J Therm Anal Calorim* **2018**, *134* (1), 209–231. https://doi.org/10.1007/s10973-018-7663-3.
(13) Munishkina, L. A.; Fink, A. L. Fluorescence as a Method to Reveal Structures and Membrane-Interactions of Amyloidogenic Proteins. *Biochimica et Biophysica Acta (BBA) -Biomembranes* **2007**, *1768* (8), 1862–1885. https://doi.org/10.1016/j.bbamem.2007.03.015.
(14) Perez, A. A.; Andermatten, R. B.; Rubiolo, A. C.; Santiago, L. G. β-Lactoglobulin Heat-Induced Aggregates as Carriers of Polyunsaturated Fatty Acids. *Food Chemistry* **2014**, *158*, 66–72. https://doi.org/10.1016/j.foodchem.2014.02.073.
(15) Pawar, S. K.; Jaldappagari, S. Interaction of Repaglinide with Bovine Serum Albumin: Spectroscopic and Molecular Docking Approaches. *Journal of Pharmaceutical Analysis* **2019**, *9* (4), 274–283. https://doi.org/10.1016/j.jpha.2019.03.007.
(16) Zhao, S.; Deng, Y.; Yan, T.; Yang, X.; Xu, W.; Liu, D.; Wang, W. Explore the Interaction between Ellagic Acid and Zein Using Multi-Spectroscopy Analysis and Molecular Docking. *Foods* **2022**, *11* (18), 2764. https://doi.org/10.3390/foods11182764.
(17) Protein Fluorescence. In *Principles of Fluorescence Spectroscopy*; Lakowicz, J. R., Ed.; Springer US: Boston, MA, 2006; pp 529–575. https://doi.org/10.1007/978-0-387-46312-4_16.
(18) Ghosh, N.; Mondal, R.; Mukherjee, S. Inverse Temperature Dependence in Static Quenching versus Calorimetric Exploration: Binding Interaction of Chloramphenicol to β-Lactoglobulin. *Langmuir* **2015**, *31* (29), 8074–8080. https://doi.org/10.1021/acs.langmuir.5b02103.
(19) Ma, T.; Zhang, L.; Xu, L.; Ye, Y.; Huang, T.; Zhou, Q.; Liu, H. Mitigation of Isoquercitrin on β-Lactoglobulin Glycation: Insight into the Mechanisms by Mass Spectrometry and Interaction Analysis. *International Journal of Biological Macromolecules* **2020**, *155*, 1133–1141. https://doi.org/10.1016/j.ijbiomac.2019.11.080.
(20) Bai, J.; Ma, X.; Sun, X. Investigation on the Interaction of Food Colorant Sudan III with Bovine Serum Albumin Using Spectroscopic and Molecular Docking Methods. *Journal of Environmental Science and Health, Part A* **2020**, *55* (6), 669–676. https://doi.org/10.1080/10934529.2020.1729616.
(21) Fa, M.; Bergström, F.; Hägglöf, P.; Wilczynska, M.; Johansson, L. B.-Å.; Ny, T. The Structure of a Serpin–Protease Complex Revealed by Intramolecular Distance Measurements Using Donor–Donor Energy Migration and Mapping of Interaction Sites. *Structure* **2000**, *8* (4), 397–405. https://doi.org/10.1016/S0969-2126(00)00121-0.
(22) Pulgarín, J. A. M.; Molina, A. A.; Ferreras, F. M. Simultaneous Determination of Doxycycline and Chlortetracycline in Real Samples by Europium-Sensitized Luminescence. *Appl Spectrosc* **2013**, *67* (4), 371–378. https://doi.org/10.1366/12-06776.

(23) Peng, W.; Ding, F.; Peng, Y.-K.; Jiang, Y.-T.; Zhang, L. Binding Patterns and Structure–Affinity Relationships of Food Azo Dyes with Lysozyme: A Multitechnique Approach. *J. Agric. Food Chem.* **2013**, *61* (50), 12415–12428. https://doi.org/10.1021/jf4039327.
(24) Yadav, J.; Kumar, Y.; Singaraju, G. S.; Patil, S. Interaction of Chloramphenicol with Titin I27 Probed Using Single-Molecule Force Spectroscopy. *J Biol Phys* **2021**, *47* (2), 191–204. https://doi.org/10.1007/s10867-021-09573-w.
(25) Sneharani, A. H.; Karakkat, J. V.; Singh, S. A.; Rao, A. G. A. Interaction of Curcumin with β-Lactoglobulin—Stability, Spectroscopic Analysis, and Molecular Modeling of the Complex. *J. Agric. Food Chem.* **2010**, *58* (20), 11130–11139. https://doi.org/10.1021/jf102826q.
(26) Barth, A. Infrared Spectroscopy of Proteins. *Biochimica et Biophysica Acta (BBA) - Bioenergetics* **2007**, *1767* (9), 1073–1101. https://doi.org/10.1016/j.bbabio.2007.06.004.
(27) Sadat, A.; Joye, I. J. Peak Fitting Applied to Fourier Transform Infrared and Raman Spectroscopic Analysis of Proteins. *Applied Sciences* **2020**, *10* (17), 5918. https://doi.org/10.3390/app10175918.
(28) Allahdad, Z.; Khammari, A.; Karami, L.; Ghasemi, A.; Sirotkin, V. A.; Haertlé, T.; Saboury, A. A. Binding Studies of Crocin to β-Lactoglobulin and Its Impacts on Both Components. *Food Hydrocolloids* **2020**, *108*, 106003. https://doi.org/10.1016/j.foodhyd.2020.106003.
(29) Hemmateenejad, B.; Shamsipur, M.; Samari, F.; Khayamian, T.; Ebrahimi, M.; Rezaei, Z. Combined Fluorescence Spectroscopy and Molecular Modeling Studies on the Interaction between Harmalol and Human Serum Albumin. *Journal of Pharmaceutical and Biomedical Analysis* **2012**, *67–68*, 201–208. https://doi.org/10.1016/j.jpba.2012.04.012.
(30) Basu, A.; Suresh Kumar, G. Binding of Carmoisine, a Food Colorant, with Hemoglobin: Spectroscopic and Calorimetric Studies. *Food Research International* **2015**, *72*, 54–61. https://doi.org/10.1016/j.foodres.2015.03.015.
(31) Ohtomo, H.; Konuma, T.; Utsunoiya, H.; Tsuge, H.; Ikeguchi, M. Structure and Stability of Gyuba, a β-Lactoglobulin Chimera. *Protein Sci* **2011**, *20* (11), 1867–1875. https://doi.org/10.1002/pro.720.
(32) Loch, J. I.; Barciszewski, J.; Śliwiak, J.; Bonarek, P.; Wróbel, P.; Pokrywka, K.; Shabalin, I. G.; Minor, W.; Jaskolski, M.; Lewiński, K. New Ligand-Binding Sites Identified in the Crystal Structures of β-Lactoglobulin Complexes with Desipramine. *IUCrJ* **2022**, *9* (3), 386–398. https://doi.org/10.1107/S2052252522004183.
(33) Tavel, L.; Andriot, I.; Moreau, C.; Guichard, E. Interactions between Beta-Lactoglobulin and Aroma Compounds: Different Binding Behaviors as a Function of Ligand Structure. *Journal of Agricultural and Food Chemistry* **2008**, *56* (21), 10208–10217. https://doi.org/10.1021/jf801841u.
(34) Wu, S.-Y.; Pérez, M. D.; Puyol, P.; Sawyer, L. β-Lactoglobulin Binds Palmitate within Its Central Cavity*. *Journal of Biological Chemistry* **1999**, *274* (1), 170–174. https://doi.org/10.1074/jbc.274.1.170.